IEEE Access
Multidisciplinary : Rapid Review : Open Access Journal

Received 15 October 2024, accepted 6 November 2024, date of publication 13 November 2024, date of current version 4 December 2024.

Digital Object Identifier 10.1109/ACCESS.2024.3497144

RESEARCH ARTICLE

Output Characteristics of a GaAs Photoconductive Semiconductor Switch With Comb Electrodes

YONG PYO KIM[1], PYEUNG HWI CHOI[1], JONGBAE KANG[2], SUNG-MIN HONG[1], (Senior Member, IEEE), SUNGBAE LEE[2], AND JAE-HYUNG JANG[2], (Senior Member, IEEE)

[1]School of Electrical Engineering and Computer Science, Gwangju Institute of Science and Technology (GIST), Gwangju 61005, Republic of Korea
[2]Department of Energy Engineering, Korea Institute of Energy Technology (KENTECH), Naju-si 58330, Republic of Korea

Corresponding author: Jae-Hyung Jang (jjang@kentech.ac.kr)

This work was supported in part by Korea Institute of Energy Technology (KENTECH) Research under Grant KRG2021-01-011, in part by the ''Regional Innovation Mega Project'' Program through Korea Innovation Foundation funded by the Ministry of Science and ICT under Project 2023-DD-UP-0015, in part by the National Research and Development Program through the National Research Foundation of Korea (NRF) funded by Ministry of Science and ICT under Grant 2022M3I8A2078705, and in part Korea Institute of Energy Technology Evaluation and Planning (KETEP) Grant funded by Korea Government through MOTIE (GAMS Convergence Course for Intelligent Electricity Safety Human Resources) under Grant 20224000000100.

ABSTRACT GaAs photoconductive semiconductor switches (PCSSs) with comb electrodes were fabricated on semi-insulating GaAs. A pulsed 1064-nm laser with a 700-ps (FWHM) pulse width and optical energy of 134 μJ was used to trigger 2-mm-gap PCSSs with comb lengths ranging from 0 to 750 μm. The effect of the comb electrodes on the output characteristics was investigated by comparing the performance parameters of sample devices with different comb lengths. Devices with a longer comb exhibited higher peak output voltage and better immunity against surface flashover. A PCSS specimen with a 750-μm comb exhibited a higher peak output voltage by 3.53 times compared to a PCSS without a comb at bias voltages lower than 1 kV. Moreover, the PCSS with the 750-μm comb electrode successfully generated a pulse with a peak voltage of 1.34 kV, while the peak voltage generated by a PCSS without a comb was limited to 0.74 kV.

INDEX TERMS Gallium arsenide (GaAs), photoconductive semiconductor switch (PCSS).

I. INTRODUCTION

Photoconductive semiconductor switches (PCSSs) have been investigated for pulsed power systems since the early 1970s [1]. High-voltage pulse generators, such as Marx generators and high-frequency antennas and pulsed microwave sources can utilize photoconductive semiconductor switches [2], [3]. The GaAs PCSS has garnered significant scientific and technical interest due to its numerous inherent advantages, including its ultrafast response, low jitter [4] and superior repetition capabilities compared to conventional switches such as the insulated gate bipolar transistor (IGBT) [5] and thyristor and spark gap switches [6].

The performance of the PCSS has been evaluated in terms of several parameters, such as the rise time, pulse width, repetition frequency, flashover voltage, and on-state resistance. The semiconductor switches for high-power pulse applications such as ultra-wideband microwave sources, ultrasound sources, laser drivers, narrow pulse width and high repetition rate are crucial to achieve high resolution and high speed pulsed power system performance [7], [8]. The flashover voltage is related to the operating voltage and lifetime of a PCSS [9]. The on-state resistance plays a crucial role in determining voltage drop and output efficiency.

The on-state resistance of a PCSS is influenced by the optical trigger energy [10], [11], [12], bias voltage, on-state current [13], trigger position [14], and the perimeter/gap ratio of the electrodes [15].

The performance capabilities of PCSS devices were compared with various electrode structures, including conventional, annular, and interdigitated types, and distinctive characteristics were observed for the devices operated at low voltages (10 V) [16]. Under 3.4 eV illumination from a Xe arc lamp, the on-state current of the devices increased linearly with the electrode width-to-gap ratio. Devices with interdigitated electrode structures and with an electrode width-to-gap ratio of 200 demonstrated 2.5-times higher on-state current than those with conventional and annular electrode

The associate editor coordinating the review of this manuscript and approving it for publication was Shuo Sun.

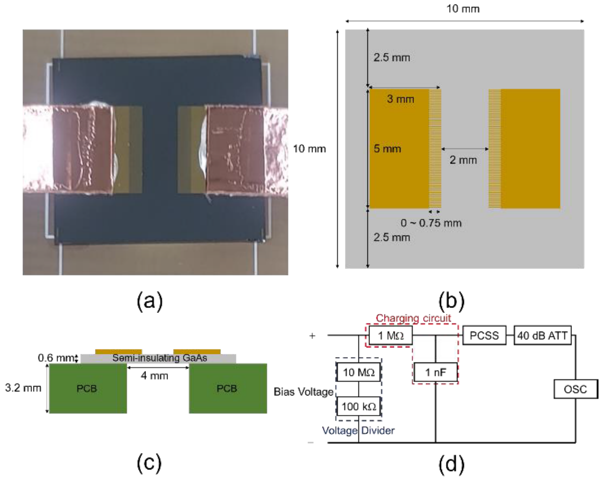

FIGURE 1. **(a) Lateral GaAs PCSS with a 2-mm gap and comb electrodes. (b) Top view and (c) side view of the device with geometric dimensions in millimeters. (d) Experimental setup to measure the output performance of the PCSS. (ATT: attenuator, OSC: oscilloscope).**

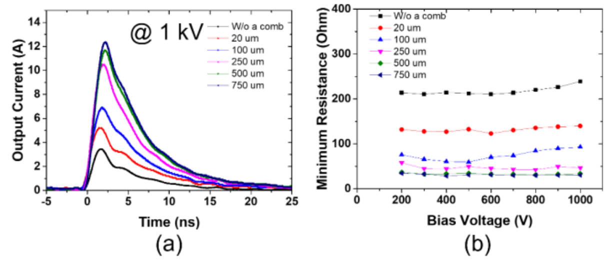

FIGURE 2. **(a) Waveforms of GaAs PCSS devices with comb lengths ranging from 0 to 750 μm. (b) Minimum resistance versus the bias voltage.**

structures [16]. However, the interdigitated structure inherently features small gaps, which limit its operation to low voltages [17]. Research on the effect of the electrode width on the on-resistance and flashover voltage in PCSS devices with millimeter-scale gaps has not yet been conducted.

In this work, lateral GaAs PCSS devices employing comb-patterned electrodes were fabricated on semi-insulating GaAs substrates. The comb-patterned electrodes are placed with a 2-mm gap, and the comb lengths range from 0 to 750 μm. By comparing the performance of the devices with various comb-length, the effect of the comb-patterned electrode on the on-state resistance and the operating voltages are investigated. By introducing comb-pattern in the electrodes of PCSS devices, the on-resistance was reduced, and the operating voltage can be increased by suppressing the flashover at the surface of the devices.

II. DEVICE FABRICATION AND EXPERIMENTAL SETUP

The PCSS tested here was fabricated on a semi-insulating (SI) GaAs substrate for which the resistivity exceeded $10^7\ \Omega \cdot$ cm and the electron mobility was greater than 5000 $cm^2\ V^{-1}s^{-1}$. Electrode metallization with Ge/Au/Ni/Au (37/100/15/200 nm) was accomplished by electron beam evaporation, with the specimen then sintered at 310 °C for 1 minute.

The fabricated device and its dimension are shown in Figs. 1(a) and (b), respectively. The gap between the electrodes is fixed to be 2 mm, regardless of the comb length in the electrodes. The comb at the edge of the electrodes has a spacing of 20 μm and a width of 20 μm with variable lengths of 0, 20, 100, 250, 500, and 750 μm.

The PCSS device is mounted on a printed circuit board (PCB) with a 4-mm-wide aperture, as shown in Fig. 1(c). For the optical triggering of the GaAs PCSS, a 1064-nm pulsed laser with a FWHM (full width at half maximum) of 700 ps and a repetition rate of 10 Hz is used. The energy of the Gaussian laser beam with a beam diameter of 2.3 mm is 135 μJ, which is monitored by an energy meter (Coherent EnergyMax J-10MB-LE).

The GaAs PCSS is tested using the circuit shown in Fig. 1(d). A high-voltage supply charges a 1 nF ceramic capacitor through a 1 MΩ resistor. In this case, 10 MΩ and 100 kΩ resistors serve as voltage dividers to monitor the bias voltage. The output voltage is attenuated by a 50-Ω terminated 40 dB attenuator (ATT) and recorded by an oscilloscope (Tektronix DPO7254) with an input impedance of 50-Ω and a band width of 2.5 GHz.

III. RESULTS AND DISCUSSION

The output characteristics of devices with variable comb structures (0, 20, 100, 250, 500, and 750 μm) are compared in Fig. 2(a). The electrical pulse width is much larger than the optical laser pulse width because the carrier lifetime in the semi-insulating GaAs used to fabricate the devices is on the order of nanoseconds [18] that is much longer than the laser pulse width of 700 ps. The PCSS remains conductive even after the laser is off, leading to an electrical pulse width that is much greater than that of the optical trigger pulse.

The GaAs PCSS with the longer comb length exhibits higher output voltage. When we compare the output voltages of the devices with the 750-μm-comb pattern and without comb-pattern, the device with comb exhibits 3.53 times greater peak output voltage. The peak output voltages of the devices with 750-μm-comb and without comb are 608 V and 172 V, respectively. The illuminated area of the PCSS with 750-μm-comb is 1.19 times larger than that of the PCSS without a comb, and the illuminated energy for the PCSS devices with 750-μm comb (97.95 μJ) is 1.20 times higher than that for the PCSS without a comb (81.92 μJ). For this calculation, Gaussian beam shape of the excitation laser is also considered. Taking into account the difference in incident light energy, it can be concluded that the devices with 750-μm comb will exhibit 2.94 times (3.53/1.20) higher output pulse compared to the PCSS without a comb if the illumination energy is same for both types of devices.

Fig. 2(b) shows the minimum resistance versus the bias voltage for PCSS devices with various comb lengths. The minimum resistance of the PCSSs tends to decrease as the comb length increases, but saturation behavior arises for the device with long comb lengths such that the devices with comb lengths of 500 and 750 μm exhibit nearly identical characteristics.

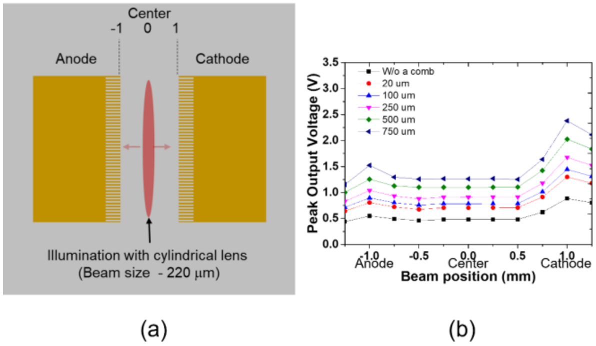

FIGURE 3. **(a) Schematic diagram showing a PCSS illuminated by an elliptical laser beam. (b) Peak output voltage versus the laser beam position for PCSS devices with various comb lengths.**

The reduced minimum on-resistance of PCSS can be attributed to two primary factors: the increase in photogenerated carriers due to a higher number of absorbed photons, and the increased effective contact width. As the comb length increases, the area illuminated by the laser beam also increases, resulting in an enhancement of the output current due to the larger number of photons incident on the GaAs surface, which was discussed earlier.

Another factor contributing to the lower device resistance is the larger effective contact width. For the PCSS without a comb, the contact width is 5 mm. In contrast, for the 750-μm comb PCSS with 125 combs, the effective contact width becomes 192.5 mm ($5+0.75 \times 125 \times 2$), which is 38.5 times greater than that of the PCSS without a comb.

To analyze whether and to what degree the comb electrodes reduce the on-state resistance, the peak output voltage was measured when the laser beam was moved from the anode to the cathode at 200 V with optical energy of 10.8 μJ. The laser beam is transformed into an ellipse with a width of 220 μm using a cylindrical lens (piano-convex cylindrical lens with a focal length of 75.2 mm), as shown in Fig. 3(a). The peak output voltage versus the beam position is shown in Fig. 3(b). When the laser illuminates the center of the device, the peak output voltage increases as the comb length increases. The peak output voltage of the PCSS with the 750-μm comb was 2.59 times higher than that of the PCSS without a comb.

Without a cylindrical lens and at a bias voltage of 200 V, the PCSS without a comb produces an output voltage of 37.65 V. In contrast, the 750-μm-comb PCSS generates a higher output of 115.35 V, which is 3.06 times greater. Considering that the PCSS with the 750-μm comb receives 1.2 times more illumination, and assuming a linear relationship between the output voltage and the optical energy, the expected increase in output voltage is 2.54 times when the same amount of optical energy is illuminated.

When the laser illuminates the edge of the cathode, the highest output voltage is observed. As the trigger position moves from the cathode towards the center of the device, the output voltage of the PCSS decreases, as demonstrated in earlier work [19]. This is attributed to the diffusion current caused by the carrier concentration gradient [19].

Surface flashover may occur under an electric field (< 10 kV/cm) much lower than the intrinsic breakdown field

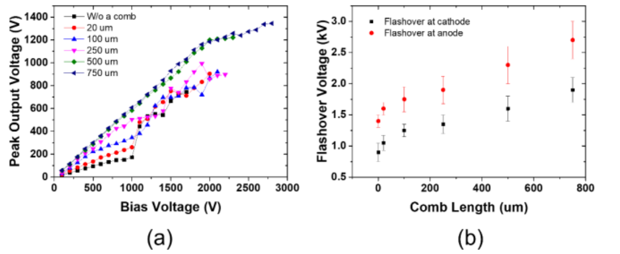

FIGURE 4. **(a) Peak output voltages versus bias voltages for PCSSs with various comb structures. For each bias voltage, 100 measurements were conducted. (b) The voltage where the flashover takes place at the cathode and the anode for devices with different comb-patterned electrodes. For each comb-length, 15 devices were measured.**

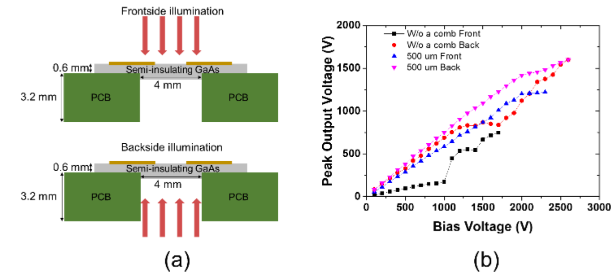

FIGURE 5. **(a) Schematic diagram showing front-side and backside illumination. (b) Peak output voltage versus the bias voltage for PCSSs with and without a comb under front-side and backside illumination conditions.**

of GaAs (250 kV/cm) [20], [21], [22]. A large number of photogenerated carriers not only results in Joule heating but also alters the electric field distribution [23].

Surface flashover begins to occur near the cathode electrode due to the high electric field caused by hole accumulation. When the PCSS is operated at higher voltages, flashover at the anode occurs, resulting in the formation of multiple cracks in the gaps between the electrodes [24], [25].

As shown in Fig. 4(a), the PCSS employing the longer comb electrodes exhibits higher output voltages. As shown in Fig. 4(b), the PCSS with the longer comb can be operated at the higher bias voltage without flashover. The PCSS without a comb exhibits anode flashover when operated at a bias voltage higher than 1.4 kV, and the device was destroyed after several operations. Meanwhile, the PCSS with the 750-μm comb can operate at a bias voltage of 2.7 kV without flashover.

The effect of backside illumination was also investigated in the device with the 500-μm comb, as shown in Fig. 5. As shown in Fig. 5(a), the laser beam enters through a 2-mm gap between the electrodes for front-side illumination, whereas the laser beam enters through the 4-mm-wide aperture of the PCB for backside illumination. The PCSS with the comb exhibits higher output voltage than the device without a comb for both front-side and backside illumination. At a bias voltage of 1 kV, the 500-μm-comb PCSS under backside illumination produces a peak voltage of 750 V, which is 1.28 times higher than the voltage of 583 V produced by the front-side illumination. For the PCSS without a comb, the peak voltage under backside illumination is 688 V, which is four times higher than the voltage of 172 V obtained under front-side illumination. The operating voltage of the devices was also higher for backside illumination compared to front-side illumination. The backside-illuminated PCSS with the 500-μm comb exhibited an operating voltage of 2.6 kV, which was higher than the operating voltage of 2.3 kV observed under front-side illumination. The enhanced output characteristics of the back-side illuminated devices are due to the reduced resistance underneath the metal contact [26], which is caused by the photo-generated carriers underneath the contact electrodes. This resistance reduction improves the overall performance of the device [27]. Additionally, these photo-generated carriers reduce the electric field intensity at the edges of the electrodes, which helps to suppress the surface flashover [28], and ensure a more even distribution of potential, thereby enabling the device to operate at higher voltages.

IV. CONCLUSION

A The effects of comb electrodes on the output characteristics of GaAs PCSS devices were investigated. A PCSS with a comb achieved a peak output voltage 3.53 times higher than that of a PCSS without a comb at a voltage level lower than 1 kV. Furthermore, the PCSS with the comb electrode demonstrated a higher operating voltage (2.8 kV) that was also higher than that (1.7 kV) of the PCSS without a comb. With backside illumination, the device performance was improved further in terms of the on-resistance as well as the operating voltage. This performance enhancement is attributed to the reduced resistance as well as the weaker field strength at the edge of the electrode metallization area due to the use of the comb electrode and the backside illumination strategy.

REFERENCES

[1] D. H. Auston, ‘‘Picosecond optoelectronic switching and gating in silicon,’’ *Appl. Phys. Lett.*, vol. 26, no. 3, pp. 101–103, Feb. 1975, doi: 10.1063/1.88079.

[2] K. Piwowarski, ‘‘Comparison of photoconductive semiconductor switch parameters with selected switch devices in power systems,’’ *Opto-Electron. Rev.*, vol. 28, no. 2, pp. 74–81, 2020.

[3] J. S. H. Schoenberg, J. W. Burger, J. S. Tyo, M. D. Abdalla, M. C. Skipper, and W. R. Buchwald, ‘‘Ultra-wideband source using gallium arsenide photoconductive semiconductor switches,’’ *IEEE Trans. Plasma Sci.*, vol. 25, no. 2, pp. 327–334, Apr. 1997, doi: 10.1109/27.602507.

[4] F. J. Zutavern, G. M. Loubriel, D. L. McLaughlin, M. W. O'Malley, W. D. Helgeson, and G. J. Denison, ‘‘GaAs PCSS: High gain switching and device reliability,’’ *Opt. Act. Switch. III*, vol. 1873, pp. 50–54, 1993.

[5] C. Luan, J. Zhao, L. Xiao, Q. Yang, X. Ma, and H. Li, ‘‘All solid-state electromagnetic pulse simulator based on the 4H-SiC photoconductive semiconductor switch,’’ *Rev. Scientific Instrum.*, vol. 91, no. 1, pp. 1–26, Jan. 2020.

[6] L. Hu, J. Su, R. Qiu, and X. Fang, ‘‘Ultra-wideband microwave generation using a low-energy-triggered bulk gallium arsenide avalanche semiconductor switch with ultrafast switching,’’ *IEEE Trans. Electron Devices*, vol. 65, no. 4, pp. 1308–1313, Apr. 2018, doi: 10.1109/TED.2018.2802642.

[7] L. Pecastaing, J. Paillol, T. Reess, A. Gibert, and P. Domens, ‘‘Very fast rise-time short-pulse high-voltage generator,’’ *IEEE Trans. Plasma Sci.*, vol. 34, no. 5, pp. 1822–1831, Oct. 2006, doi: 10.1109/TPS.2006.883346.

[8] X. Chu, J. Liu, T. Xun, L. Wang, H. Yang, J. He, and J. Zhang, ‘‘MHz repetition frequency, hundreds kilowatt, and sub-nanosecond agile pulse generation based on linear 4H-SiC photoconductive semiconductor,’’ *IEEE Trans. Electron Devices*, vol. 69, no. 2, pp. 597–603, Feb. 2022, doi: 10.1109/TED.2021.3138950.

[9] G. M. Loubriel, F. J. Zutavern, A. G. Baca, H. P. Hjalmarson, T. A. Plut, W. D. Helgeson, M. W. O'Malley, M. H. Ruebush, and D. J. Brown, ‘‘Photoconductive semiconductor switches,’’ *IEEE Trans. Plasma Sci.*, vol. 25, no. 2, pp. 124–130, Apr. 1997, doi: 10.1109/27.602482.

[10] H. Ekinci, V. V. Kuryatkov, D. L. Mauch, J. C. Dickens, and S. A. Nikishin, ‘‘Plasma etching of n-Type 4H-SiC for photoconductive semiconductor switch applications,’’ *J. Electron. Mater.*, vol. 44, no. 5, pp. 1300–1305, May 2015.

[11] B. Wang, K. Liu, and J. Qiu, ‘‘Analysis of the on-state resistance influenced by the on-state current,’’ in *Proc. IEEE Int. Power Modulator High Voltage Conf. (IPMHVC)*, Jun. 2012, pp. 649–652, doi: 10.1109/IPMHVC.2012.6518828.

[12] T. Zhang, K. Liu, S. Gao, and Y. Shi, ‘‘Characteristics of GaAs PCSS triggered by 1 μJ laser diode,’’ *IEEE Trans. Dielectr. Electr. Insul.*, vol. 22, no. 4, pp. 1991–1996, Aug. 2015, doi: 10.1109/TDEI.2015.004950.

[13] J. Wei, F. Zeng, H. Chen, L. Wang, S. Li, and B. Qian, ‘‘Analyses of the on-state resistance of a coplanar GaAs PCSS in the nonlinear mode,’’ in *IEEE MTT-S Int. Microw. Symp. Dig.*, Nov. 2022, pp. 1–3, doi: 10.1109/IMWS-AMP54652.2022.10106982.

[14] Y. Sun, L. Hu, X. Dang, L. Zhu, X. Yang, J. Huang, Y. Li, and X. Li, ‘‘Investigation on the mechanism of triggering efficiency of high-power avalanche GaAs photoconductive semiconductor switch,’’ *IEEE Electron Device Lett.*, vol. 42, no. 11, pp. 1646–1649, Nov. 2021, doi: 10.1109/LED.2021.3114600.

[15] A. R. Chowdhury, J. C. Dickens, A. A. Neuber, R. Ness, and R. P. Joshi, ‘‘Lock-on physics in semi-insulating GaAs: Combination of trap-to-band impact ionization, moving electric fields and photon recycling,’’ *J. Appl. Phys.*, vol. 123, no. 8, pp. 1–26, Feb. 2018.

[16] A. D. Koehler, T. J. Anderson, A. Khachatrian, A. Nath, M. J. Tadjer, S. P. Buchner, K. D. Hobart, and F. J. Kub, ‘‘High voltage GaN lateral photoconductive semiconductor switches,’’ *ECS J. Solid State Sci. Technol.*, vol. 6, no. 11, pp. S3099–S3102, 2017.

[17] M. Xu, X. Liu, M. Li, K. Liu, G. Qu, V. Wang, L. Hu, and H. Schneider, ‘‘Transient characteristics of interdigitated GaAs photoconductive semiconductor switch at 1-kHz excitation,’’ *IEEE Electron Device Lett.*, vol. 40, no. 7, pp. 1136–1138, Jul. 2019, doi: 10.1109/LED.2019.2916427.

[18] B. R. Holeman and C. Hilsum, ‘‘Photoconductivity in semi-insulating arsenide gallium,’’ *J. Phys. Chem. Solids*, vol. 22, pp. 19–24, 1961.

[19] B. Wang, T. Zhang, K. Liu, and J. Qiu, ‘‘Characteristics of the GaAs photoconductive semiconductor switch operated in linear-alike mode,’’ *IEEE Trans. Electron Devices*, vol. 60, no. 8, pp. 2580–2585, Aug. 2013, doi: 10.1109/TED.2013.2266928.

[20] L.-M. Wang, ‘‘Relationship between the intrinsic breakdown field and the bandgap of materials,’’ *Microelectron*, vol. 36, no. 6, pp. 576–579, 2006.

[21] X. Chu, T. Xun, L. Wang, J. Liu, H. Yang, J. He, and J. Zhang, ‘‘Breakdown behavior of GaAs PCSS with a backside-light-triggered coplanar electrode structure,’’ *Electronics*, vol. 10, no. 3, p. 357, Feb. 2021.

[22] C. Ruan, W. Zhao, S.-L. Zhu, H.-J. Liu, H.-C. Yang, and C.-L. Ruan, ‘‘Characterization of photoconductive semiconductor switches under a nonlinear mode condition,’’ *Microw. Opt. Technol.*, vol. 51, no. 1, pp. 56–59, 2009.

[23] S. Wang and W. Shi, ‘‘The role of the photo-generated carrier in surface flashover of the GaAs photoconductive semiconductor switch,’’ *IEEE J. Electron Devices Soc.*, vol. 6, pp. 179–182, 2018, doi: 10.1109/JEDS.2017.2783898.

[24] C. Ma, W. Shi, M. Li, H. Gui, L. Wang, H. Jiang, Z. Fu, and J. Cao, ‘‘Research on flashover characteristics and the physical mechanism of high-gain GaAs photoconductive switches,’’ *IEEE J. Quantum Electron.*, vol. 50, no. 7, pp. 568–574, Jul. 2014, doi: 10.1109/JQE.2014.2327191.

[25] G. M. Loubriel, F. J. Zutavern, A. Mar, H. P. Hjalmarson, A. G. Baca, M. W. O'Malley, W. D. Helgeson, R. A. Falk, and D. J. Brown, ‘‘Longevity of optically activated, high gain GaAs photoconductive semiconductor switches,’’ *IEEE Trans. Plasma Sci.*, vol. 26, no. 5, pp. 1393–1402, Oct. 1998, doi: 10.1109/27.736024.

[26] C. Y. Chang, Y. K. Fang, and S. M. Sze, ‘‘Specific contact resistance of metal-semiconductor barriers,’’ *Solid-State Electron.*, vol. 14, no. 7, pp. 541–550, Jul. 1971.

[27] Y. P. Kim, P. H. Choi, M.-S. Kim, J. Ryu, S.-H. Baek, S.-M. Hong, S. Lee, and J.-H. Jang, ‘‘Photoresponses of the back-side illuminated GaAs photoconductive semiconductor switches in the linear mode,’’ *Solid-State Electron.*, vol. 164, Feb. 2020, Art. no. 107680.

[28] G. M. Loubriel, M. W. O'Malley, F. J. Zutavern, B. B. McKenzie, and W. R. Conley, ‘‘Surface flashover threshold and switched fields of photoconductive semiconductor switches,’’ in *Proc. Annu. Report., Conf. Electr. Insul. Dielectric Phenomena*, Oct. 1988, pp. 430–441, doi: 10.1109/CEIDP.1988.26369.